The true potentials and transition barriers at dislocations

2002 J. Phys.: Condens. Matter 14 12801

(http://iopscience.iop.org/0953-8984/14/48/319)

INSTITUTE OF PHYSICS PUBLISHING JOURNAL OF PHYSICS: CONDENSED MATTER

J. Phys.: Condens. Matter **14** (2002) 12801–12811 PII: S0953-8984(02)54043-1

The true potentials and transition barriers at dislocations

R Labusch

Institute of Physics and Physical Technology, Technical University Clausthal, Germany and Department of Physics, University of Natal, Durban 4001, South Africa

E-mail: r.labusch@t-online.de

Received 27 September 2002
Published 22 November 2002
Online at stacks.iop.org/JPhysCM/14/12801

Abstract

The classical logarithmic potential of a charged dislocation which is widely used in the analysis of electrical and optical properties, determination of dislocation-associated levels, etc, can be significantly modified due to, among other effects, the deformation potential of the strain field as well as to the graininess of the screening charge cloud as long as it consists of shallow impurities.

In general, this reduces the effective potential barrier to carrier recombination, the activation energy for thermal emission of trapped non-equilibrium carriers from core states, and also the optical excitation energies for transitions from the core into free band states.

These effects are discussed in some detail and general rules concerning their relative importance are established.

1. Line charges and screening clouds

Dislocations in semiconductors are usually modelled as charged lines that are surrounded by a cylinder of screening charges which compensate the line charge with the result that the sum of all charges is zero.

In the early work on this topic (Read 1954) the dislocation core was described as a row of acceptor-like dangling bond (DB) states which are localized at a distance b from each other. For 60° dislocations which are often the predominant type after plastic deformation as well as in mismatch networks of epitaxial layers, b happens to be equal to the length of the Burgers vector. If a fraction f of the DBs are occupied, the line charge per unit length of dislocation is $q = ef/b$.

Later on, after the presentation of convincing evidence from carrier density measurements on Ge (Schröter 1967, Schröter and Labusch 1969, Labusch and Schröter 1978), it was concluded that the core states in this material are actually one-dimensional bands, i.e. they are non-localized, the charge density is homogeneous along the dislocation, and the line charge

is smeared out over a cylinder of radius r_i which is given by the extent of the wavefunction perpendicular to the line direction. r_i is of the order of b. This view has been confirmed by direct measurements of one-dimensional conduction along dislocation lines (Hess and Labusch 1993).

On the other hand, the core states in Si seem to be localized at points on the line which can be either intrinsic defects (for instance jogs) or impurities (single atoms or small precipitates) that have been scavenged by the dislocation or segregated in or near the core (Kronewitz 1991, Kveder *et al* 2001, Schröter and Cerva 2002). For the sake of convenience we continue to use the description of the line charge in terms of f and b although only $q = ef/b$ has a direct physical meaning. The true occupation of core states is then $f^*(b/c)$ where c is the actual distance between point defects at the core.

The screening cloud was described in the early work as a cylinder of charged shallow impurities (Read 1954). The charge density inside this cylinder is

$$\rho = eN_{\mathrm{sh}} \qquad \text{for } r < r_0$$

and zero outside r_0. The screening radius r_0 is given by the neutrality condition:

$$\pi r_0^2 N_{\mathrm{sh}} = f/b.$$

We call this CI screening.

As an alternative, the screening can be described as a partial expulsion of free carriers from the vicinity of the dislocation (Schröter 1967, Schröter and Labusch 1969, Labusch and Schröter 1978). We call this FC screening. The charge density in this case is continuous:

$$\rho \propto \exp(-r/\lambda); \qquad \lambda = \sqrt{\frac{\varepsilon\varepsilon_0 kT}{e^2 n_{\mathrm{free}}}}.$$

In most experiments, the free carrier density is approximately equal to the density of shallow impurities N_{sh}. Actually both types of screening are always present, but usually CI screening predominates at high occupation and/or low temperatures.

The transition from CI to FC screening can be estimated in two ways:

(i) From the condition $U_{\mathrm{core}} = kT$ where U_{core} is the electrostatic potential of the charged line and the screening cloud at the core. From this, anticipating an expression for the potential (see below), we obtain by elementary algebra $f_{\mathrm{tr}} = kT/[W_{\mathrm{coul}} \ln(r_0/r_i)]$ for the occupation at the transition.

$$W_{\mathrm{coul}} = \frac{e^2}{2\pi\varepsilon\varepsilon_0 b}$$

is a characteristic electrostatic energy of the problem which will be used throughout this paper. Its values are 0.68 and 0.45 eV for Si and Ge, respectively. $\ln(r_0/r_i)$ typically takes on values between 2 and 7.

(ii) From the condition that the screening radius is greater or less than the screening length λ. With the expressions for r_0 and λ given above, we obtain $f_{\mathrm{tr}} = kT/2W_{\mathrm{coul}}$. This is somewhat higher than the value according to (i). For f between these two values, we have CI screening close to the dislocation and FC screening at larger distances, and with increasing f an increasing fraction of the screening charge is contained in the CI regime. Typical values of f_{tr} according to (ii) are in the range from 0.5 to 1.5%. In most experiments, except near neutrality, i.e. $f = 0$, CI screening is predominant.

2. Calculation of the electrostatic potential

Assuming CI screening and localized line charges, the electrostatic potential is given by

$$U_{\mathrm{elst}} = W_{\mathrm{coul}} \frac{1}{2} \left(\sum_{\ell} \frac{1}{|\vec{x} - \vec{x}_\ell|} - \sum_{s} \frac{1}{|\vec{x} - \vec{x}_s|} \right)$$

where $\vec{x}_\ell$ and $\vec{x}_s$ refer to the positions of charged defects in the dislocation core and in the screening cloud, respectively. Normalizing all lengths by b/f we obtain

$$U_{\mathrm{elst}} = W_{\mathrm{coul}} f G(\vec{r}, R)$$

where $\vec{r}$ is now the normalized vector of the point at which the potential is calculated and

$$R = r_0 f/b = \sqrt{\frac{f^3}{\pi N_{\mathrm{sh}} b^3}}$$

is the normalized screening radius. The range of R is typically from 20 to 200. In the temperature range of interest, FC screening takes over if f becomes small enough and/or N_{sh} big enough to render R smaller than 20.

$G(\vec{r}, R)$ can be considered as a normalized potential and depends only of the type of screening and the arrangement of the charges in the dislocation core. The following calculations are mainly concerned with this function.

For the sake of simplicity we shall assume equidistant charges in the dislocation core but keep in mind that, at elevated temperatures, fluctuations of the distances are expected. The corresponding contribution to the electrostatic potential is of the order of kT (Read 1954, Broudy and McClure 1960). As a consequence of the normalization, the distance between charges on the line as well as the volume density of charged impurities are unity in the calculations that follow.

A simple approximate solution for the electrostatic potential is obtained if both the line charge and the screening are assumed to be homogeneous and if the distance to the core is greater than unity in normalized units:

$$G = \ln(R/r) - \frac{1}{2}\left[1 - \left(\frac{r}{R}\right)^2\right] \qquad \text{(Read 1954).} \tag{1}$$

In a numerical calculation for discrete line charges we notice that there is a significant difference between

(i) the potential of an electron approaching a site between two charged points on the line, which is the position of lowest energy (the 'between sites' position), and
(ii) that of an electron which is taken away from an occupied site, mainly because the distance to the nearest-neighbour charges in the 'on-site' position is twice as large as that in the 'between' position.

Figure 1 shows the calculated normalized potentials for $R = 25$ and 150 for both positions, together with the potential according to equation (1). We notice that the difference of the curves for different R is practically constant as predicted by equation (1), but that the curves for discrete line charges are significantly different from each other and from equation (1). The relative difference is of course inversely proportional to the absolute value and therefore maximal for small R. The difference between the 'on-site' and the 'between sites' positions extends to large radii. This is understandable because an electron that is taken away from the line leaves behind an empty site. Whether this has physical consequences will be discussed later on.

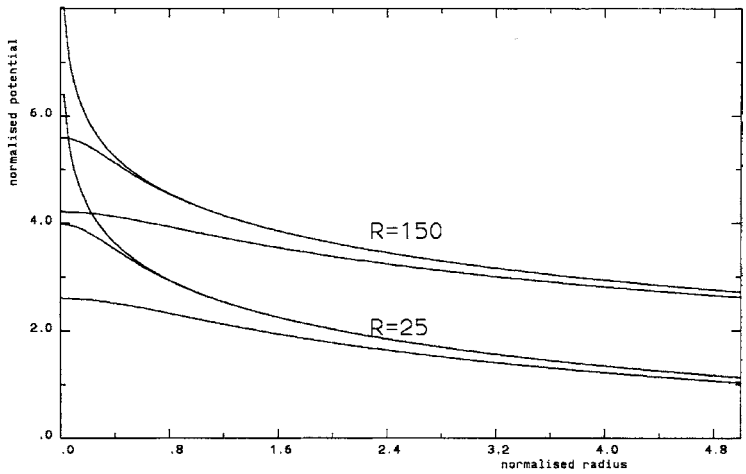

Figure 1. The electrostatic potential of a dislocation line for two values of the normalized screening radius. Here, as in the other figures, the potential is normalized by $W_{\mathrm{coul}} f$. The upper group of three curves was calculated for $R = 150$, the lower group for $R = 25$. In each group the uppermost curve represents the simplified potential given by equation (1), the middle curve corresponds to the 'between' position, and the lowest curve corresponds to the 'on-site' position.

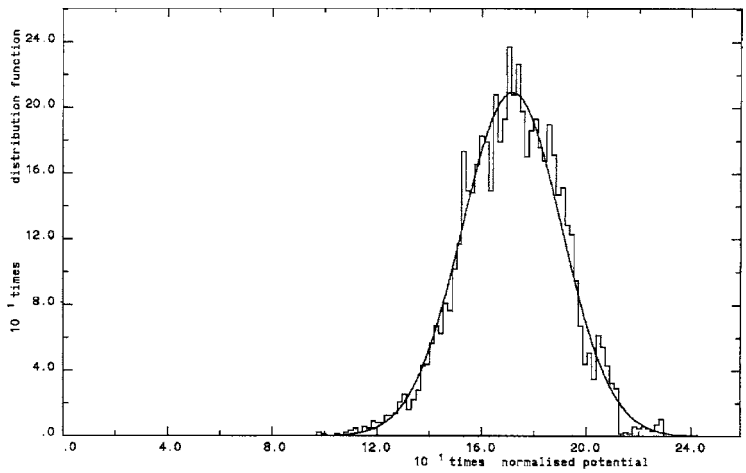

Figure 2. The distribution of electrostatic potential values in the dislocation core, assuming a constant line charge. The smooth curve is a Gaussian distribution with the same half-width. The screening radius in this example is $R = 20$. The half-width varies approximately proportionally to the inverse square root of R. Fluctuations of the actual potential are reduced by readjustment of the line charge.

3. Fluctuations

If the line charge per unit length in the core is constant, screening by a statistical array of charged shallow impurities leads to fluctuations of the potential. This was simulated in a numerical calculation. Figure 2 shows the distribution of potential values near the core obtained from 4000 different random distributions, together with a Gaussian of the same variance. The screening radius in this calculation was $R = 20$ (in normalized units). The width of the distribution

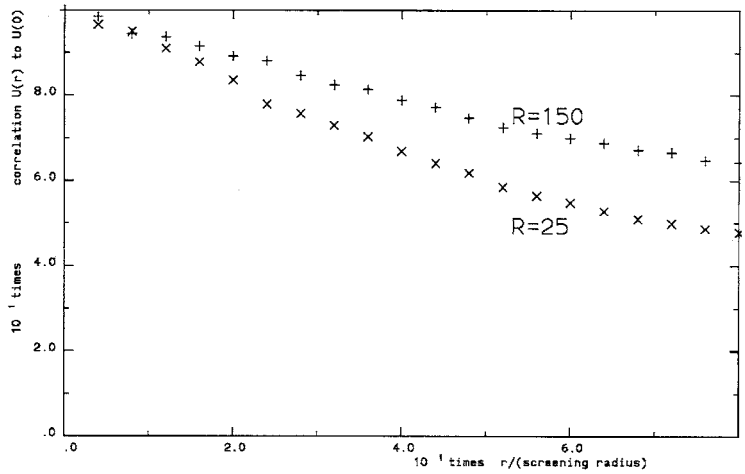

Figure 3. The correlation between the electrostatic potential fluctuations at the normalized distance r/R from the core and in the core (see figure 2) for $R = 25(\times)$ and $R = 150(+)$.

function decreases roughly with the inverse square root of R. At first sight, the simulation seems to indicate that, at the lower end of the range of R, fluctuations can be significant. However, we have to take into account that the occupation of the core states depends on the local value of the potential and the potential in turn depends on occupation f:

$$\delta U_{\text{core}} = W_{\text{coul}} f\, \Delta G(0, R) + W_{\text{coul}} f \left(\frac{1}{f} + \frac{\partial G}{\partial f} \right) \delta f. \tag{2}$$

Only the first term on the right-hand side of this equation is calculated in the simulation for constant f.

If the core states are acceptors with a single level, the change of f with U_{core} is given by $\frac{\delta f}{f} \approx -\frac{\delta U_{\text{core}}}{kT}$. Combining this with equation (2) we obtain

$$\delta U_{\text{core}} = W_{\text{coul}} f\, \Delta G(0, R) \frac{1}{1 + W_{\text{coul}} f \left(G + f \frac{\partial G}{\partial f} \right) / kT},$$

so δU_{core} is smaller than $kT\, \Delta G/G$ and therefore may be safely neglected. This negative feedback of the occupation on variations of the core potential has also been noticed by other authors (Kveder *et al* 2001) in a different context. We conclude that, because of their long range, significant fluctuations are expected only in the occupation of the core states and not in the potential around the dislocation.

In the next section we show that the barrier to transitions to and from the dislocation core states does not coincide with the core position but is situated up to a few normalized units away from it. To check that the negative feedback is nevertheless valid, we have evaluated by simulation the correlation between the potential values at distance r from the core and at the core. The result is shown in figure 3 as a plot of

$$\text{correlation} = \frac{\langle (U(0, R) - \langle U(0, R) \rangle)(U(r, R) - \langle U(r, R) \rangle) \rangle}{\sqrt{\langle (U(0, R) - \langle U(0, R) \rangle)^2 \rangle} \sqrt{\langle (U(r, R) - \langle U(r, R) \rangle)^2 \rangle}}$$

versus r/R for $R = 25$ and 100. The figure shows that the correlation is very close to unity (more than 90%) for distances up to $2R$, so within the range of expected barrier positions the fluctuations contribute no more to the barrier height than to the core potential and may be neglected as well.

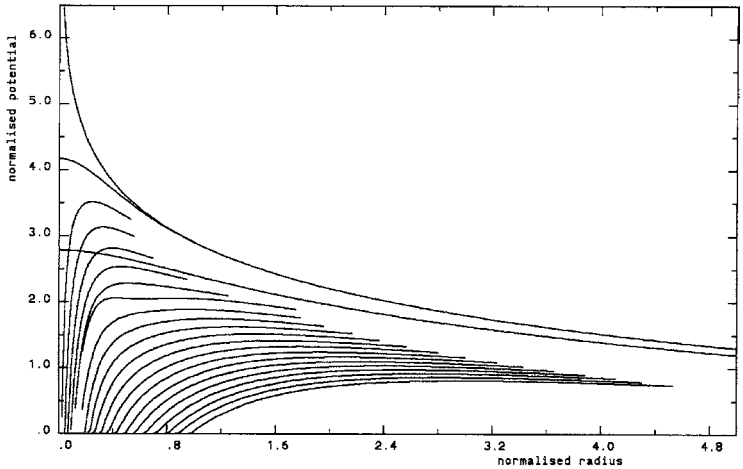

Figure 4. Numerical calculation of the normalized sum of electrostatic and deformation potentials in the 'on-site' position as a function of the normalized radius r at a 60° dislocation. Both partials are taken into account in the deformation potential. r is taken in the direction of the saddle point. The normalized screening radius is $R = 30$. The set of curves represents values of the deformation potential strength D^* from 0.1 to 2.0; a group of curves for the normalized electrostatic potential, as in figure 1, are given for reference.

4. Activation barriers

In the early work on dislocations, the barrier to transitions from the conduction band into dislocation core states was assumed to be given by the height of the core potential. Later on, it was suggested that the effective barrier height is significantly reduced by tunnelling through the top of the potential near the core (Schröter 1967). This effect is particularly strong if the wavefunction of the core is non-local along the line but well localized in the perpendicular direction, which seems to be true for Ge. In this case the uppermost curves in figure 1 which have very pointed tips are valid, and the inner cut-off radius to be inserted in equation (1) is of the order of f in normalized units (b in normal units). On the other hand, tunnelling is expected to be less effective for localized charges in the core because the top of the potential curve is flat.

More recently, it has been suggested that the deformation potential of the dislocation strain field can reduce the barrier significantly versus the pure electrostatic potential (Hess 1994, Labusch 1997).

The deformation potential is given by the deformation potential tensor as

$$U_{\mathrm{def}} = \sum_{ij} \Xi_{ij}\varepsilon_{ij}.$$

Predominant in the sum are the terms connected with a change of the nearest-neighbour distance and, consequently, with the strength of the covalent bonds. The corresponding components of Ξ are negative. U_{def} is therefore essentially proportional to the edge component of the Burgers vector and changes sign across the glide plane of the dislocation.

In the coordinate system which is sketched in figure 4, the deformation potential of a pure edge dislocation is then to a fair approximation

$$U_{\mathrm{def}} = -\frac{b_{90^\circ} D}{2\pi r}\cos(\phi) \qquad \text{where } D \approx -\Xi_{yy} > 0.$$

A more comprehensive treatment, using isotropic elasticity theory, of the potential at a particular dislocation (the partial surrounding a Ni precipitate in Si) has been worked out by Hedemann and Schröter (1997).

Unfortunately the components of the deformation potential are difficult to measure and their values not well known. The best values available at present are $D = 10$ eV for Ge and $D = 6$ eV for Si (Landolt–Börnstein 1982). These may be subject to revision if better data become available and also if corrections due to elastic anisotropy are taken into account. In the present situation, we shall carry out calculations with D as a parameter.

Our workhorse, the 60° dislocation, is dissociated into a 90° partial for which the Burgers vector has the length $b_{90°} = b/\sqrt{3}$ and a 30° partial whose edge component is $b_{30° \text{ edge}} = \frac{1}{2}b/\sqrt{3}$.

The deformation potential gives rise to bound states (one-dimensional bands) that split off from the band edges of the bulk into the gap (Winter 1977, 1978, Alexander and Teichler 2000). From calculations, the binding energies of these states turn out to be rather small, not much bigger than those of shallow impurities. But one should expect the binding energy to be somewhat modified by the presence of the dislocation core which cannot be described in terms of a deformation potential. Evidence for the existence of a rather shallow one-dimensional band in Si has been obtained from AC conductivity measurements after saturating the core states with atomic hydrogen (Kveder *et al* 1985), from microwave conductivity measurements (Brohl *et al* 1990), and also from the photoluminescence at dislocations (Kveder *et al* 1995, 2001).

We also expect some contribution of the deformation potential to the energy of the core states.

For core states and shallow bands it is important to notice that by definition the dislocation levels are always related to the unperturbed band edges of the bulk and that their position is not affected by the deformation potential, whereas the electrostatic potential shifts the core levels and the shift is practically equal to the potential value.

In a simplified preliminary analysis, only the deformation potential of the 90° partial was taken into account and equation (1) was used for the electrostatic potential (Labusch 1997). The total potential is then

$$U = W_{\text{coul}} f \left\{ \ln(R/r) - \frac{1}{2}\left(1 - \left(\frac{r}{R}\right)^2\right) - \frac{D^*}{r}\cos(\phi) \right\}.$$

In this expression we have introduced our normalized length unit b/f and extracted the factor $W_{\text{coul}} f$. The strength of the deformation potential is represented by

$$D^* = \frac{b_{90°} D}{b W_{\text{coul}}}.$$

With the above-mentioned D-values, the values of D^* are 2 and 0.8 for Ge and Si, respectively. U has a saddle point in the direction $\phi = 0$ at $r_{\text{saddle}} = D^*$ and the value of U at the saddle point is reduced relative to the core value at the inner cut-off radius r_i by

$$U_{\text{core}} - U_{\text{saddle}} = W_{\text{coul}} f \{\ln(D^*/r_i) + 1\}.$$

For Ge, because of its large D^* and small r_i ($r_i \approx f$ in normalized units), this is always a large fraction of U_{core}, but even for Si it is not negligible at the lower end of the range of R.

In a more elaborate numerical evaluation, we take into account the contribution of the 30° partial which is not really negligible compared with that of the 90° partial.

Furthermore, we do the calculation for discrete core charges and for the two positions ('on' and 'between' sites) that were mentioned before.

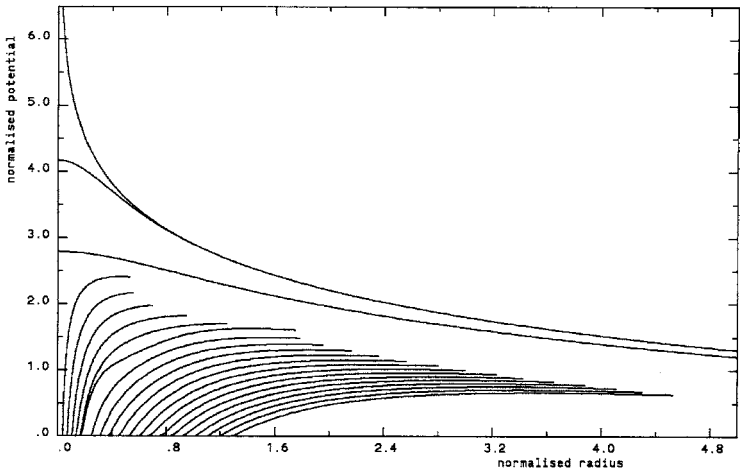

Figure 5. The normalized sum of the electrostatic and deformation potentials in the 'between sites' position. Otherwise the same as figure 4.

Unfortunately, since the results depend on the separation of the partials, we need another parameter besides R and D^* in the calculation. In our example, which is presented in figures 4 and 5, we have assumed a stacking fault width of 5 nm and $N_{sh} = 5 \times 10^{14}$. The screening radius is $R = 30$. Each set of curves represent D^*-values between 0 (uppermost curve) and 2 (lowest curve) for the 'between' (figure 4) and 'on-site' positions (figure 5). The electrostatic potentials shown in figure 1 are repeated for reference. The results for different values of the screening radius have practically the same appearance and are merely shifted against those of figures 4 and 5 by a nearly constant value $\approx \ln(R/30)$ as may be expected from the simplified form of the potential. The results show that, certainly for Ge but even for Si, the activation barrier can be significantly lower than the potential in the core.

In principle, the barrier can be further reduced if a charged impurity happens to be in a position close to the saddle point but far enough from the core that the negative feedback via the local occupation of core states is not or only partially effective. From our correlation analysis it follows that this must be a rare exception. Qualitatively, one would expect the probability of obtaining this situation for one of the 'on-site' or 'between' positions to be roughly $1/R^2$. This is always so small that no significant reduction of the barrier due to a charged impurity is expected on any relevant dislocation segment (length: a few microns). This was in fact confirmed directly by a simulation of 10 000 sites with different random arrays of screening charges. Only at three of these was the barrier reduced by more than 10%, due to the presence of a screening charge close to the saddle point.

Inspecting the results in figures 5 and 6, we have to keep in mind that both the starting position of a transition from the core to a free bulk state and the final relaxed end position of a transition from a free state to the core are 'on site' at $r = 0$. In the latter case, the charges in the core have to go through a relaxation process in which the 'between sites' position becomes 'on site'. A relaxation of the total energy of the system is also possible for the reverse process, because the removed electron leaves behind a gap in the line charges that will eventually collapse and turn into an equidistant distribution for which the potential of the free electron is now 'between sites'.

It has been suggested that, as a rule, because the transition is very slow, the hopping rate of charges along the line is faster than the transition rate to and from the core (Figielski 1990).

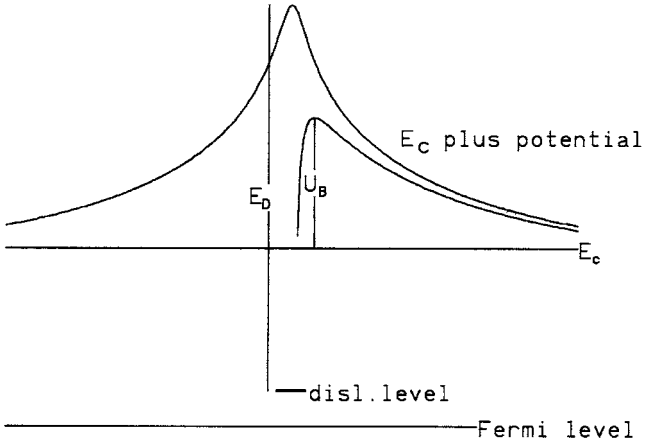

Figure 6. A schematic drawing of the levels, the electrostatic potential, and the barrier at dislocations.

This seems to suggest that the relaxation of charges in the core takes place during the transition. If this is accepted, the effective potential, both ways, should be an interpolation between 'on site' and 'between sites'. However, although this approach appears quite plausible in a particle picture, the following line of arguments which is based on wave mechanics casts considerable doubt on its validity. Consider for instance the transition of a free electron to a core state. The transition is slow because free states at the energy of the saddle point are rarely occupied; but once an electron has collected enough energy, the quantum mechanical transition is *fast*. Furthermore, before the transition has taken place, there is no driving force for the subsequent relaxation process which is expected to happen only *after* the extra electron in the core has been localized in the middle between to other charges. A similar reasoning can be applied to the reverse process: the relaxation by which the gap in the charge distribution is filled and an equidistant minimum energy distribution re-established can take place only *after* the transition.

We therefore leave the different potentials as they are given in the figures, but have to admit that a true many-body treatment of the transition process which includes also fluctuations of the charge positions in the dislocation core would be desirable. We notice that for small D^* the barrier for a transition into the dislocation core can be higher than the potential of an electron in the 'on-site' position to which it relaxes *after* the transition.

5. Thermal activation analysis

Frequently, the analysis of experiments is done by means of an Arrhenius plot and determination of an activation energy Q from its slope. With reference to figure 6, the rate of transition across the saddle point in n-type material is proportional to $\exp\left(-\frac{U_B+(E_C-\mu)}{kT}\right)$, where U_B is the potential at the saddle point, E_C the edge of the conduction band, and μ the Fermi level. Generally the activation energy in the exponent is not independent of T. If the dependence is assumed to be linear, it is cancelled by the denominator, so Q is the extrapolated value at $T = 0$:

$$Q = \lim_{T\to 0}[U_B + (E_C - \mu)].$$

If we furthermore assume $U_B = U_{core}$, a constant carrier density in the experimental temperature range, and an acceptor-like core level, the final result is $Q = E_D$. This follows

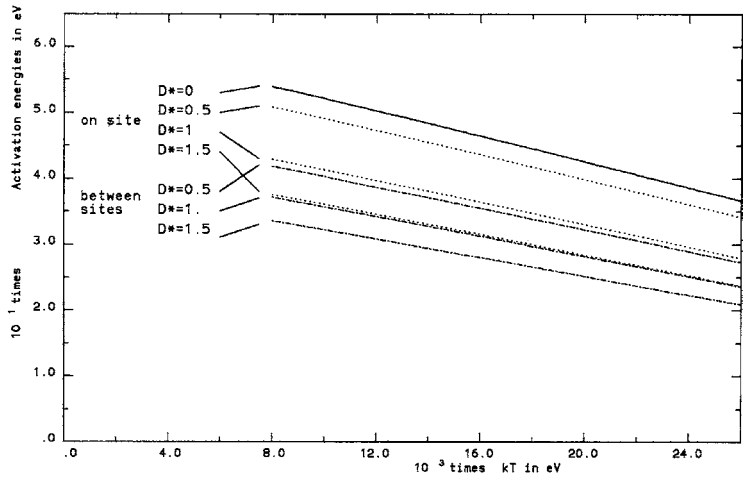

Figure 7. Thermal activation analysis of rates of transition to and from dislocation states. The uppermost curve shows $[U_{\text{core}} + (E_{\text{C}} - \mu)]$ as a function of temperature T in the 'on-site' position. It is equal to the activation barrier for $D^* = 0$. The other curves represent the barrier in the 'on-site' position (dotted lines) and the 'between sites' position (dashed lines) for values of the deformation potential strength $D^* = 0.5$, 1.0, and 1.5. The measured activation energy Q (the slope of an Arrhenius plot) is obtained by linear extrapolation from the experimental range of T to $T = 0$.

because at $T = 0$, the Fermi level is pinned to the dislocation level which remains at E_{D} below the local level of the conduction band edge.

If, on the other hand, $U_{\text{B}} < U_{\text{core}}$ while the other assumptions remain valid, we obtain

$$Q = \lim_{T \to 0} [E_{\text{D}} - (U_{\text{C}} - U_{\text{B}})]$$

No general formula is available for the quantitative dependence of $(U_{\text{C}} - U_{\text{B}})$ on T which comes about through the dependence on $f(T)$. It has to be evaluated separately for each case under investigation by numerical calculation. Nevertheless, it can be useful to consider a typical example which illustrates the expected features of the correct solutions and the quality of simplifying assumptions such as the linearity in temperature. For this purpose, $U_{\text{B}} + (E_{\text{C}} - \mu)$ and $U_{\text{core}} + (E_{\text{C}} - \mu)$ were calculated as functions of T under the assumptions $N_{\text{sh}} = 5 \times 10^{14}$ and $E_{\text{D}} = 0.6$ eV.

The Fermi level was obtained from

$$n = N_{\text{sh}} = CT^{3/2} \exp[-(E_{\text{C}} - \mu)/kT]$$

and inserted in

$$f = \frac{1}{1 + \exp[(E_{\text{C}} - \mu + U_{\text{core}} - E_{\text{D}})/kT]}$$

to obtain $f(T, U_{\text{core}})$. The numerical $U_{\text{core}}(f)$ was then inserted in this equation and it was solved for f which was then inserted into $U_{\text{core}}(f)$ and $U_{\text{B}}(f)$. The result is shown in figure 7. The uppermost curve is $U_{\text{core}} + (E_{\text{C}} - \mu)$ which is independent of D^* and equal to the activation barrier for $D^* = 0$. As mentioned before, U_{core} is taken in the 'on-site' position.

The other three pairs of curves represent parameter values of the normalized strength D^* of the deformation potential between 0.5 and 1.5. In each pair the upper and the lower curve are $[U_{\text{B}} + (E_{\text{C}} - \mu)]_{\text{between sites}}$ and $[U_{\text{B}} + (E_{\text{C}} - \mu)]_{\text{on site}}$, respectively.

The following conclusions can be drawn from an inspection of this figure:

(i) The linearity is not perfect for either plot, but is sufficient to render the thermal activation analysis a useful tool.
(ii) $\lim_{T\to 0}[U_{\mathrm{core}} + (E_{\mathrm{C}} - \mu)]$ is close to E_{D}.
(iii) $Q = \lim_{T\to 0}[U_{\mathrm{B}} + (E_{\mathrm{C}} - \mu)]$ is significantly reduced with respect to E_{D} for Ge ($D^* = 2$), and even for Si ($D^* = 0.8$) the reduction is not negligible.

References

Alexander H and Teichler H 2000 *Handbook of Semiconductor Technology* vol 1, ed K A Jackson and W Schröter (New York: Wiley–VCH) p 291
Broudy R M and McClure J W 1960 *J. Appl. Phys.* **31** 1511
Brohl M, Dressel M D, Helberg H W and Alexander H 1990 *Phil. Mag.* B **61** 97
Figielski T 1990 *Phys. Status Solidi* a **121** 187
Hedemann H and Schröter W 1997 *Solid State Phenom.* **57–58** 293
Hess J 1994 *PhD Thesis* Clausthal University
Hess J and Labusch R 1993 *Phys. Status Solidi* a **138** 617
Hess J, Schreiber J, Hildebrand S and Labusch R 1992 *Phys. Status Solidi* b **172** 225
Kronewitz J 1991 *Thesis* Göttingen University
Kveder V, Kittler M and Schröter W 2001 *Phys. Rev.* B **63** 115208
Kveder V, Labusch R and Ossipyan Yu A 1985 *Phys. Status Solidi* a **92** 293
Kveder V, Steinman E A, Shevchenko S A and Grimmeiss H G 1995 *Phys. Rev.* B **51** 10520
Labusch R 1997 *J. Physique* III **7** 1411
Labusch R and Schröter W 1978 *Dislocations in Solids* vol 5, ed F R N Nabarro (Amsterdam: North-Holland) p 127
1982 *Landolt–Börnstein New Series* Group III, vol 17 (Heidelberg: Springer)
Read W T 1954 *Phil. Mag.* **45** 775
Read W T 1954 *Phil. Mag.* **45** 1119
Schröter W 1967 *Phys. Status Solidi* **21** 211
Schröter W and Cerva H 2002 *Solid State Phenom.* **85–86** 67
Schröter W and Labusch R 1969 *Phys. Status Solidi* **36** 539
Winter S 1977 *Phys. Status Solidi* b **79** 637
Winter S 1978 *Phys. Status Solidi* b **85** K95
Winter S 1978 *Phys. Status Solidi* b **90** K289